Pilot Relaying Scheme Based on Differential Admittance Concept for FSC-Compensated EHV Transmission Line

Piyush Khadke[1] · Nita Patne[2] · Arvind Singh[3] · Gulab Shinde[4]

Abstract

This article presents a novel per-phase differential admittance (DA) concept-based relaying scheme applied in transmission system with fixed series capacitors. For a given two-bus system, DA is defined as the difference in the sending-end and receiving-end bus admittances at a given instance. This per-phase DA relaying scheme detects, classifies and trips the faulty phase accurately with fast response. The system is modeled and validated with PSCAD/EMTDC software with real-time 400 kV system parameters, and the algorithm has been programmed in MATLAB. The global positioning system time-stamped synchronized measurement is used. Also, the proposed algorithm has been verified successfully with two-machine system hardware with real-time data. The proposed scheme uses only one-cycle moving window, sample-by-sample checking information and has a low computational burden. The benefit of this scheme is that there is no need to change relay threshold settings for uncompensated and series-compensated line. The proposed scheme is tested on a variety of fault parameters. Simulation and hardware results demonstrate the reliability, accuracy and the fast approach of the proposed scheme over other conventional schemes.

Keywords Admittance relaying · Transmission-line modeling · Fixed series compensation · Pilot relaying

1 Introduction

Modern transmission grid system demands more power transfer capability and increased voltage level for loss cutback without risking the stability of the system.

✉ Piyush Khadke
piyushkhadke88@gmail.com; khadkepm@rknec.edu

Nita Patne
nrpatne@eee.vnit.ac.in

Arvind Singh
arvindsinghwce@gmail.com

Gulab Shinde
shinde_gulab@yahoo.co.in

1 Electrical Engineering Department, Shri Ramdeobaba College of Engineering and Management, Nagpur, India

2 Electrical Engineering Department, Visvesvaraya National Institute of Technology, Nagpur, India

3 School of Electrical Engineering, Shandong University, Jinan, P. R. China

4 EHV Testing, Power Grid Corporation of India Ltd., Wardha, Maharashtra, India

Considering the right-of-way (ROW) problems and other environmental regulations and impacts, it has become a tough job to construct new transmission lines to fulfill increasing power demand (Kim et al. 2011; Kumar and Jena 2019; Rahmani et al. 2013). Various series compensation techniques are utilized to increase the power transfer capacity of a transmission corridor without compromising the system stability of the existing transmission grid. Fixed series capacitors (FSC) have been utilized as one of the beneficial means to increase power transfer and cost-effective measures over the decades. But, the presence of FSC in transmission system leads a conventional impedance-based distance relay to mal-operate numerous times, causing disruption in power and interruption in grid stability. This happens due to nonlinear high capacitive currents produced by series capacitors during abnormal conditions. Moreover, nonlinearity produced with overvoltage protection of FSC by metal oxide varistor (MOV) and spark gap in parallel to capacitors add up to the improper estimation of impedance-based distance relaying schemes during faults. As a result, protection relay of transmission line overreaches or underreaches in an

unpredictable manner (Kumar and Jena 2019; Ahmed et al. 2012; Sarangi and Pradhan 2014). Operators and designers are therefore left with the option of subsequent changes in the relay settings to overcome the undesirable effects of series compensation which is not always a practical task.

A detailed analysis of effects of series compensation on protection of transmission line and new approaches to overcome these mal-effects are presented in Vyas et al. (2014) and Chen et al. (2016). Current differential protection with steady-state phasor estimation-based approach for normal transmission line and extension to series-compensated line is presented in Dambhare et al. (2009). Reference (Bolandi et al. 2014) presents a new fault component-integrated power concept for uncompensated line protection, which is defined as the difference between pre-fault and post-fault integrated powers. However, relay threshold value settings have to be changed for series-compensated line with the scheme in Bolandi et al. (2014) which is not the issue in the proposed per-phase differential admittance (DA)-based scheme. A generalized admittance-based method for fault type and location estimation for uncompensated system has been suggested in Tan et al. (2015), but lacks to specify time response of fault detection. Admittance measurement-based inverse-time relay characteristic is proposed in Dewadasa et al. (2009) with reach setting explanation in the radial distribution network. Response time in Dewadasa et al. (2009) is much more than one cycle, whereas proposed DA-based scheme has faster response time. References (Shien et al. 2011; Suonan et al. 2011a, b; He et al. 2013a, b) introduce a new fault component-integrated impedance method for transmission system protection which is defined as the ratio of the sum of the fault component voltage phasors of the two ends of the transmission line to the sum of the current phasors of fault component of the that line. This integrated impedance concept is used to check whether the fault is inside the line or outside the line section. Reference (Hinge and Dambhare 2015) proposes secure phase comparison method for the protection of transmission line to detect faulty phase, but only 100 km line is considered for simulation purpose. The same integrated impedance concept-based protection tactic in a transmission line with static VAR compensator (SVC) compensation is given (Gupta and Tripathy 2014) but sampling frequency is not specified. References (Jena and Samantaray 2014a, b) use imaginary part of integrated impedance theory for fault classification in unified power flow controller (UPFC) and thyristor-controlled series compensation (TCSC) compensated lines, respectively, but changes in settings which are to be made in case of uncompensated line are not discussed. Reference (Jena and Samantaray 2016) proposes a differential relaying scheme for lines with UPFC in wind farms using post-fault one-cycle differential data of sequence components of two

end voltages and currents. Another relaying scheme is given in uncompensated double circuit lines in Jena and Samantaray (2015) applying phase angle of differential impedance signal to check whether the fault is internal or external. Novelty of the proposed scheme is that it overcomes all the above difficulties making it more reliable and efficient.

The proposed scheme uses a novel per-phase differential admittance concept for per-phase fault detection, fault phase classification and accurate fault phase tripping. DA is defined as the difference in per-phase sending-end and receiving-end bus admittance at a given instance. The absolute value of this DA is used to set the relaying criteria. Initially, differential impedance and conventional methods are tested in considered transmission system with FSC. Cross-tripping in nonfaulty phases and mal-operation of relays in the form of underreach or overreach are found in conventional impedance methods. Also, normal impedance-based relays give zone- or section-wise protection with time delay. In order to overcome these mentioned problems, a new all-inclusive relaying approach of DA is applied and is found to work accurately in all fault conditions. Advantage of the reduced memory requirement of admittance calculation over impedance in matrix form is also well known. This concept relay is used as a main relay in series-compensated line protection. This concept has never been used in relaying methods, making it new. Being a per-phase scheme, it works accurately in symmetric as well as asymmetric fault cases.

In this research work, the 400 kV transmission line with FSC of Western Grid of Power Grid Corporation of India Ltd. is simulated to validate the proposed scheme. It is comprised of an equivalent model of 400 kV transmission line of 400 km length with two end buses and 400 kV FSC with its parallel protection scheme based on the real system parameters of the actual installed system. Figure 1 shows the equivalent single-line representation of the proposed scheme. Two external lines are considered as shown in Fig. 1 with same line lengths and line parameters for external fault cases. *Vs, Is, Vr* and *Ir* are the sending- and receiving-end voltages and currents, respectively, of the line under consideration, and proposed relay has been considered at sending-end throughout. In practice, these measurements are done with 0.2 accuracy class current transformers (CT) and capacitive voltage transformers (CVT) for metering purpose which give highly accurate measurements and saturation effects of measuring current and voltage transformers can be avoided. Also, practical distance relays used in transmission protection system such as SEL, SIPROTIC (SIEMENS) and REL (ABB) change relay settings for different locations of compensation and even after that mal-operation is observed. However, proposed relay does not mal-operate for any location of

Fig. 1 Single-line representation of considered system
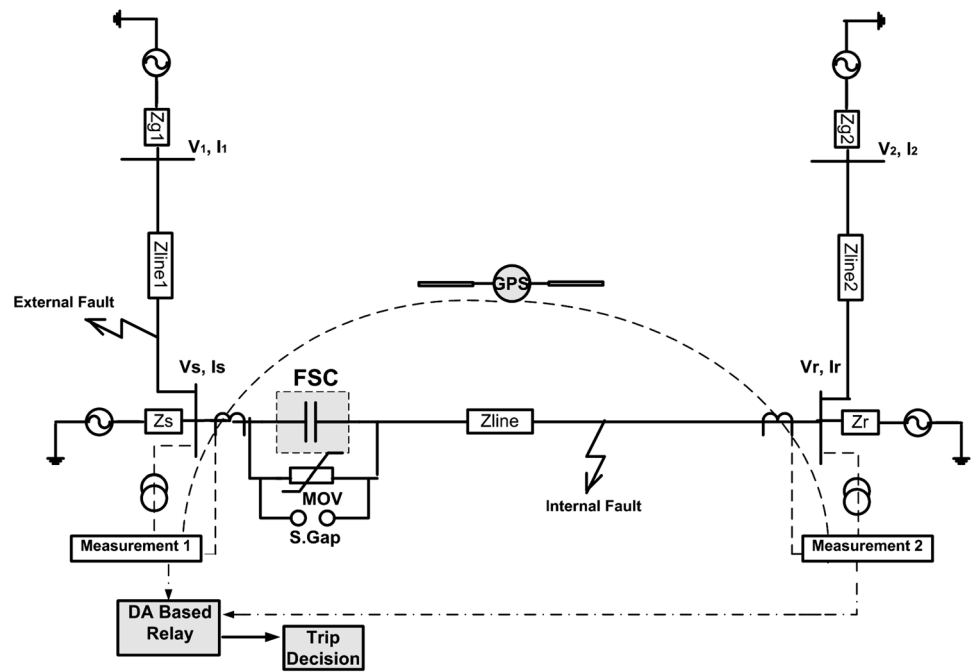
compensating device and also there is no need to change the relay setting for such cases.

Consistency of the proposed scheme is validated by extensive simulations in all types of internal and external shunt faults. Detailed fault parameters like fault distance, fault inception angle (FIA) or fault instance, fault resistance (R_f), installation position of FSC, level of compensation and load angle at bus, etc., have been varied to prove the performance reliability, accuracy and fast response of the proposed scheme. Authors have tried to build an entirely new and simple concept with easy application in the system which has proven to be fast and less complex. The superiority of the proposed scheme over other conventional schemes is given in Sect. 7.

2 Differential Admittance (DA) Concept

DA is the difference in the sending-end bus admittance and receiving-end bus admittance for a given time instance. Admittance and differential admittance (DA) in general are defined as (1) and (2), respectively,

$$Y = \left(\frac{I}{V}\right) \tag{1}$$

$$DA = Y_{send} - Y_{receive} \tag{2}$$

When the fault occurs in the transmission system, change in current and voltage is seen to be abrupt. Rate of change of fault current is very high as compared to voltage. So, significant change can be seen in differential admittance value as compared to differential impedance value. This significance has been verified with simulation analysis given in this section. In differential admittance relaying concept, consideration of even the remote-end admittance value increases the reliability of relaying and also the zone-wise operation with a time delay of conventional impedance-based distance relay can be overcome. Figure 2a, b shows the differential admittance and differential impedance comparison plots for c–g fault and a–c fault, respectively, at 0.3 s for 400 kV transmission system. It can be seen that change in differential admittance is significant only in faulty phase and fault detection criteria can be easily set. However, differential impedance graph is changing abruptly even in nonfaulty phase and fault detection is very difficult and not reliable, especially in transient time. Also, advantage of admittance over impedance usage in regard to sparsity is already a well known fact.

In this scheme, absolute value of DA has been used. Hence, setting a specific threshold value, faults in the complete line section can be detected and classified with this DA scheme correctly. As shown in Fig. 1, proposed scheme is tested for four-bus system with multiple sources for internal and external faults. As there is differential component in DA approach, the effect of changes in current contribution from external sources, infeed currents do not cross the set threshold value and hence the proposed scheme is immune to infeed effects.
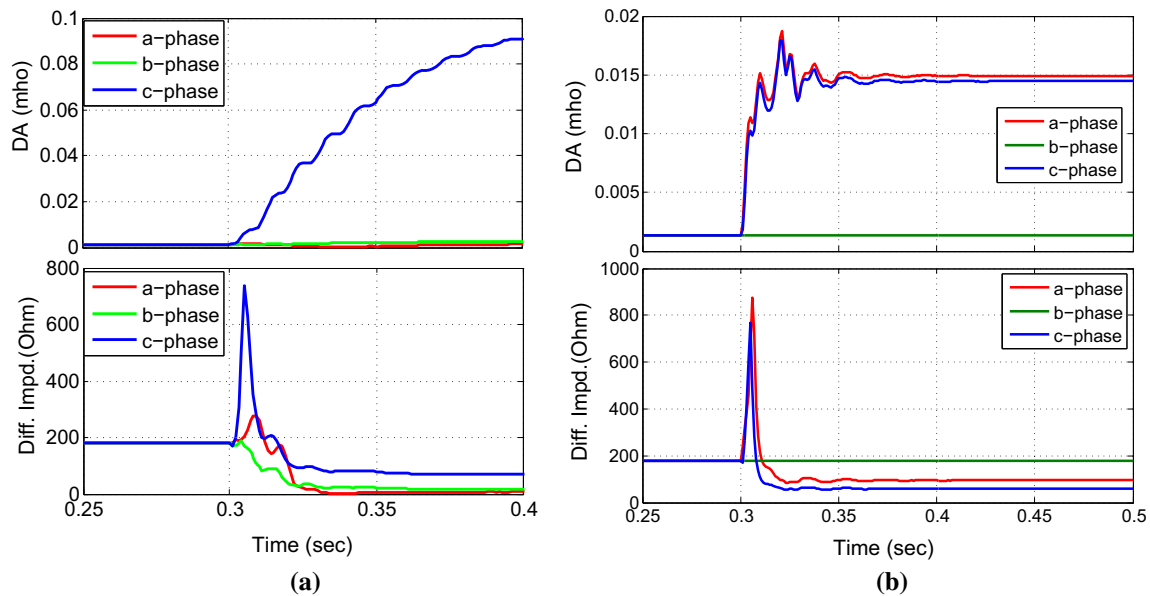
Fig. 2 DA and differential impedance comparison plots for **a** c–g fault and **b** a–c fault

3 Relaying Algorithm

A discrete sampling frequency of 1 kHz, i.e., 20 samples/cycle, is used in the simulation. Better accuracy is achieved with sample-by-sample checking in this scheme. The main structure of the proposed algorithm is described in Fig. 3. The detailed algorithm is as follows:

(1) Measure per-phase voltage and current at sending and receiving-end buses continuously by metering instruments.

(2) Pass these input signals through anti-aliasing filter, sample and hold circuit, multiplexer, analog-to-digital converter, digital filter, etc., as followed in practice. Then, apply moving-window discrete Fourier transform (DFT) to extract current and voltage phasors of both ends.

(3) Calculate per-phase admittance at both ends and transfer remote-end admittance signal to relaying end through high-speed dedicated communication link having fiber optic connectivity. These signals are GPS time-stamped.

(4) Compute per-phase DA and simultaneously per-phase absolute value, i.e., |DA|. Finally, check per-phase |DA| criterion. If |DA| > set threshold in continuous five samples, then send a trip signal to that particular phase circuit breaker (CB). Else, return to the first step. The calculated set threshold value is given in the test cases section.

Measurement of phase voltage and current is done with high-accuracy class instrument transformers. Before giving the input signals to the algorithm, these measured signals
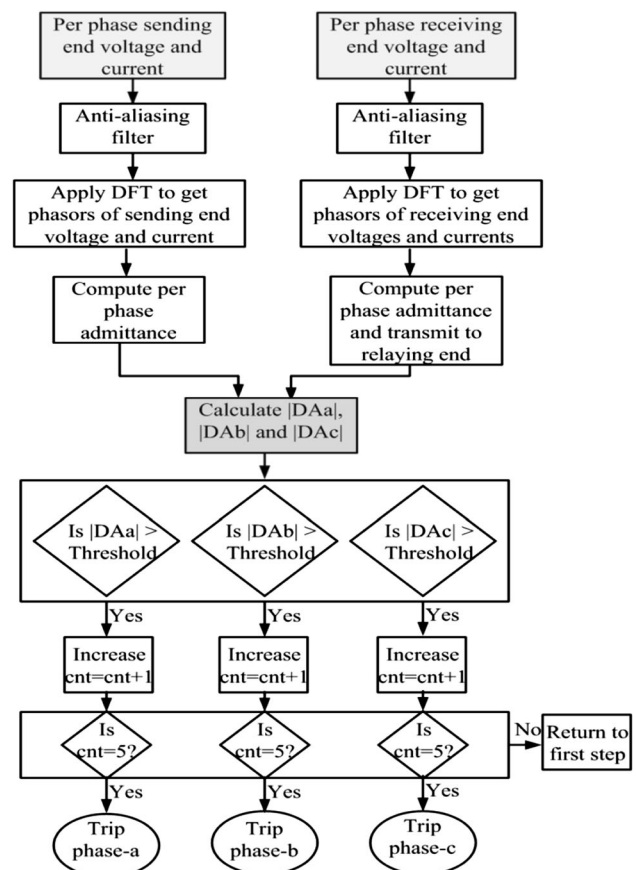

Fig. 3 Outline of the proposed relaying algorithm

are first passed through an analog low-pass anti-aliasing filter, because digital processing can take place only after the frequency spectrum of the signal is properly shaped.

Before passing to DFT stage, these signals are passed through sample and hold circuit, multiplexer, analog-to-digital converter, digital filters, etc., as followed in practice. The set threshold counter (cnt) criteria of five samples increase the operation reliability.

4 System Configuration and Test Cases

System modeling and validation is performed using PSCAD/EMTDC software. After fetching the fault set data, programming of proposed relaying scheme is done in MATLAB environment with 1 kHz sampling frequency, i.e., 20 samples/cycle. Sampling rate affects the relay operation time. It has been observed that higher sampling rate gives fastest relay operation; however, only marginal gains in speed of relay operation reduce the accuracy at higher sampling frequencies. i.e., a result in accord with the law of diminishing marginal utility (Dambhare et al. 2009). Also, higher sampling rate requires more samples to be checked to set the threshold criterion to maintain reliability of the operation which in turn will increase the computational burden. Keeping this in mind, 1 kHz sampling rate has been used for reliable and fast operation. Actual installed three-phase 400 km, 400 kV series-compensated transmission system parameters are considered for modeling. A two-end bus three-phase 400 kV, 50 Hz transmission with FSC system, as shown in Fig. 1, has been developed to test and validate the proposed scheme. The power system comprises two sources with buses, 400 km transmission line, FSC with its associated protecting components, GPS-synchronized measurement units, assuming no communication delay and proposed DA-based relay with fiber optic links for measurement data retrieving to relay. The speed of the relaying also depends on the speed of the communication channel since synchronized data are required. Newly built TLs are equipped with a high-speed communication channel (He et al. 2013a, b; Gupta and Tripathy 2015). Optical fibers with a low refractive index (approximately 1.52) are available nowadays (Gupta and Tripathy 2015). With this low refractive

index, the signal will take approximately 1.52 ms to reach the distance of 300 km. But in real practice, with a 1000-km connection, the one-way delay is roughly 4–5 ms at 2.5 Gbps (Jena and Samantaray 2014a, b). The FSC installation location is varied at sending end, midpoint and receiving end of the transmission line. The transmission-line parameters and other real-time data at bus used for simulation purpose are specified in "Appendix" section.

Total line reactance is $X_l = 107.6\ \Omega$. The capacitive reactance of FSC is $X_c = 43.04\ \Omega$ which is 40% of the total line reactance and $X_c = 26.9\ \Omega$ for 25% compensation. Maximum current rating of capacitor bank is designed for 3000 A. The maximum continuous operating voltage of the MOV is designed at 130 kV. As the MOV is a nonlinear resistive element and it has an energy dissipation limit, an overload protection is provided to protect it against excessive heat. The overload protection calculates the energy absorbed by the MOV, and a parallel spark gap is triggered if the energy crosses a threshold value, i.e., 15 MJ used for this study. The transmission line is modeled using the structural information of tower data, circuit conductor data, circuit ground wire data, circuit conductor bundling data and phase connection considering frequency-dependant phase model in PSCAD. The fault current is measured at the relaying end with ANSI 1200:5; class C400 current transformer (CT) model has been used for obtaining the realistic CT response during simulations. Also, the measurements on both the ends are GPS synchronized.

The proposed scheme has been tested in various internal and external faults like single-phase-to-ground, phase-to-phase and three-phase faults. Various fault parameters as mentioned in Table 1 are varied to test and validate the proposed scheme. The scheme testing has been performed on more than 20,000 fault cases as mentioned in Table 1.

Rigorous simulations are carried out to fix the threshold value used in the proposed scheme performing severe fault cases like realistic fault resistance, fault location very near to FSC as well as far away from FSC with sudden power loading changes at bus during various fault instances. In case of high fault resistance fault cases, change in fault

Table 1 Fault parameters

Variation	Range
FSC position	Bypass mode, sending end, midpoint and receiving end
Type of fault	a–g, b–g, c–g, a–b, b–c, a–c, a–b–g, b–c–g, a–c–g and 3-ph
%Compensation	25% and 40%
Fault location	5–395 km (in step of 5 km from relaying end)
R_f	0.1–300 Ω
Load angle	5°, 10°, 15°
Fault inception	0.1 s to 1 s (in step of 0.002 s)
Load encroachment	50–300 MW

current is less as compared to severe faults. In order to make this scheme sensitive to such cases also, the smaller change in the differential admittances must be considered for fault detection. The transmission line compensated with FSC is operated near to thermal limit of loading, and even a small change in fault current can damage the capacitor banks, which is not at all recommended considering the importance of the line and critical load flow. Hence, the threshold value is fixed as 0.005 for this transmission research system from knowledge experience and rigorous database. Also, to make this scheme more reliable, the threshold-crossing criteria counter is set to 5, i.e., as soon as per-phase DA value crosses the set threshold five times continuously, and then only per-phase tripping command will be issued. With this threshold counter of 5, tripping for situations of short-time disturbances which are not actual faults can be avoided. In real practice, even the distance relays have different settings according to various transmission system parameters.

5 Simulation Results

The proposed scheme was tested, and simulation results were obtained by considering all types of shunt faults with varying fault conditions. The relay location is considered at sending end as shown in Fig. 1. Further, the FSC installation locations were considered at sending end, midpoint and receiving end of the transmission line. FSC bypass normal line or uncompensated line mode was also considered. Realistic fault resistance values have been used considering the previous real-time fault data at the power grid substation. In order to validate and check performance, the proposed scheme was tested on randomly selected fault cases with various fault parameters and results are given for internal faults, external faults and other transient conditions as below.

5.1 Uncompensated (FSC Bypass) Mode

The proposed scheme was tested in this normal line mode, i.e., when FSC is in bypass or no compensation mode. One of the test case results in this mode is shown in Fig. 4. Plots of per-phase DA, i.e., DA_a, DA_b and DA_c, respectively, are shown in Fig. 4 for a single-phase a–g fault at 20 km from relaying end or sending end with $R_f = 10\ \Omega$ at fault inception of 0.3 s. It was seen that after the inception of fault, only DA values in a-phase were increased above threshold of 0.005 while the DA values in the b-phase and c-phase were below threshold. Also, as per the set threshold counter criteria of five samples, the fault was detected in a-phase at 0.307 s, i.e., in 7 ms after the inception of fault as shown in Fig. 4. This showed that the proposed
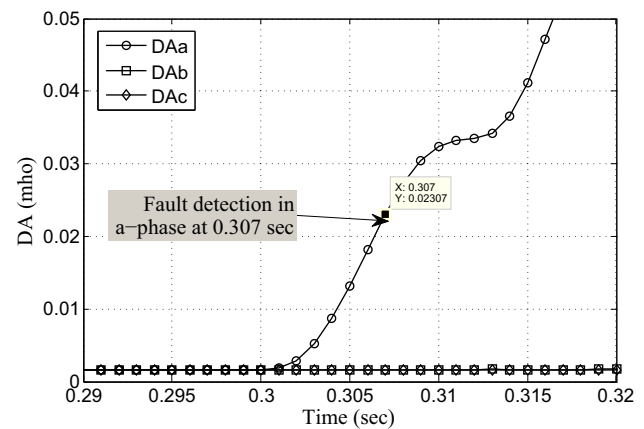

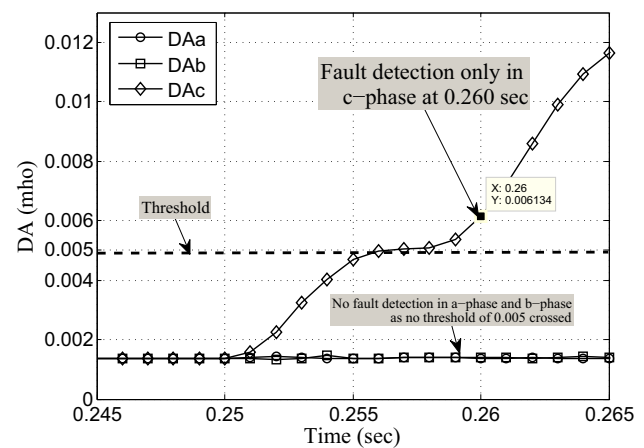**Fig. 4** Plot of per-phase DA for a–g fault at 0.3 s

Fig. 5 Plot of per-phase DA for c–g fault at 0.25 s

algorithm detected the fault accurately in a-phase only with a fast response within the half cycle time and only faulty phase was tripped.

5.2 FSC at Sending End

The proposed FSC was considered at the relaying end in this mode. Figure 5 shows the plots of per-phase DA for a single-phase c–g fault at 380 km from relaying end with $R_f = 70\ \Omega$ at fault inception of 0.25 s. It was seen that after the inception of fault, only DA values in the c-phase were increased above threshold of 0.005 while the DA values in a-phase and b-phase were below threshold. Also, as per the set threshold counter criteria of five samples; the fault was detected in the c-phase at 0.26 s, i.e., in 10 ms after the inception of fault as shown in Fig. 5. This showed that the proposed DA-based algorithm detected the fault accurately in c-phase only followed by subsequent c-phase tripping.

5.3 FSC at Midpoint

FSC was considered at midpoint of transmission line in this mode. Figure 6 shows the plots of per-phase DA for a two-phase b–c fault at 270 km from relaying end with $R_f = 5\ \Omega$ at fault inception of 0.15 s. It was seen that after the inception of fault, only DA values in the b-phase and c-phase were increased above threshold of 0.005 while the DA values in a-phase were below threshold. Also, as per the set threshold counter criteria of five samples, the fault was detected in b-phase and c-phase at 0.158 s, i.e., in 8 ms, respectively, after the inception of fault, whereas there was no fault detection in a-phase. This proved that the proposed DA-based algorithm detected the fault accurately in b-phase and c-phase only followed by subsequent two-phase tripping.

5.4 FSC at Receiving End

FSC was considered at other end of the transmission line in this mode. Figure 7 shows the plots of per-phase DA for a
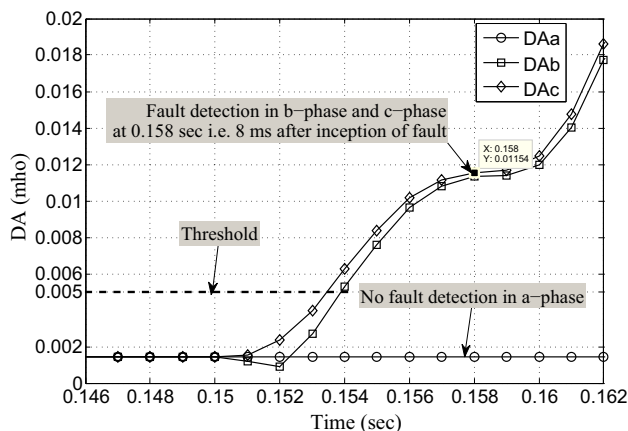

Fig. 6 Plot of per-phase DA for b–c fault at 0.15 s
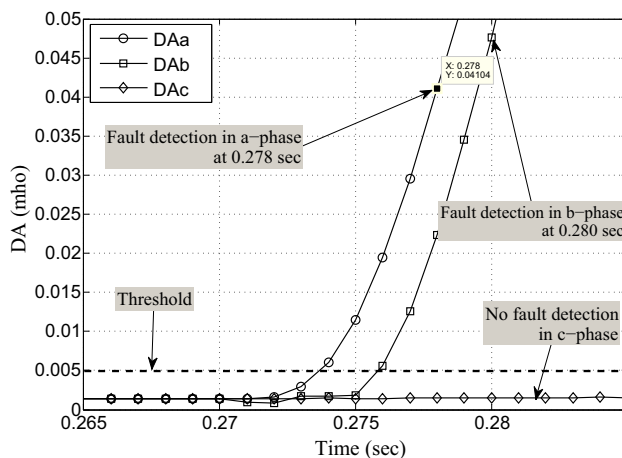

Fig. 7 Plot of per-phase DA for a–b–g fault at 0.27 s

two-phase a–b–g fault at 33 km from relaying end with $R_f = 0.1\ \Omega$ at fault inception of 0.27 s. It was seen that after the inception of fault, only DA values in a-phase and b-phase were increased above threshold of 0.005 while the DA values in the c-phase were below threshold. Also, as per the set threshold counter criteria of five counters, the fault was detected in a-phase and b-phase at 0.278 s and 0.280 s, i.e., in 8 ms and 10 ms, respectively, after the inception of fault, whereas there was no fault detection in c-phase. This proved that the proposed DA-based algorithm detected the fault accurately in a-phase and b-phase only followed by subsequent two-phase tripping.

5.5 External Fault Cases

The proposed scheme was tested for external fault cases by creating various faults outside the given line section. External faults were created in the other line sections behind the sending end and receiving end. In case of external faults, post-fault per-phase DA values were found to be well below the set threshold value and hence proposed relay did not mal-operate for external faults. Figure 8a shows the plots of per-phase DA for a–g fault at 50 km behind relaying end with $R_f = 10\ \Omega$ at fault inception of 0.25 s. Figure 8b shows the plots of per-phase DA for a–c–g fault at 118 km behind relaying end with $R_f = 100\ \Omega$ at fault inception of 0.25 s. It was seen that after the inception of fault in both the figures, all per-phase DA values were found to be well below the threshold of 0.005 and hence faults were not detected in any phase. It was also observed that the proposed scheme operated for some of the severe external faults for fault distances less than 5% of the external line lengths, i.e., very near and behind the relaying end with FSC at relaying end.

5.6 Sudden Switching of FSC

The proposed scheme was verified for test cases of sudden switching on and off of FSC capacitor banks at random instances. Even in case of normal switching on and off capacitor banks and lines, the proposed scheme did not mal-operate. The normal switching cases did not affect the proposed scheme performance. One of the test cases of sudden switching on of capacitor banks is discussed in Fig. 9. Figure 9 shows a test case of sudden insertion of capacitor bank at 0.302 s in the specified line, and it was seen that per-phase DA values were found to be well below the set threshold value and hence proposed relay did not mal-operate for this switching condition.
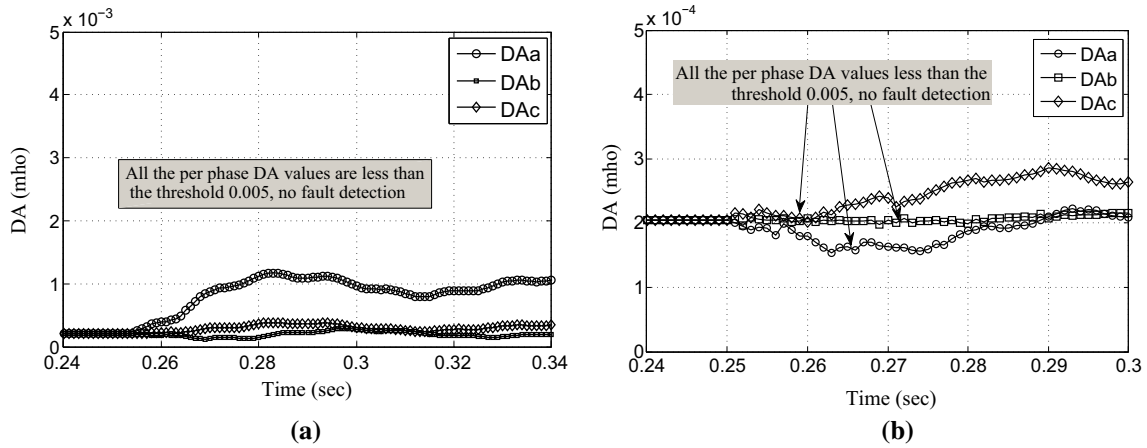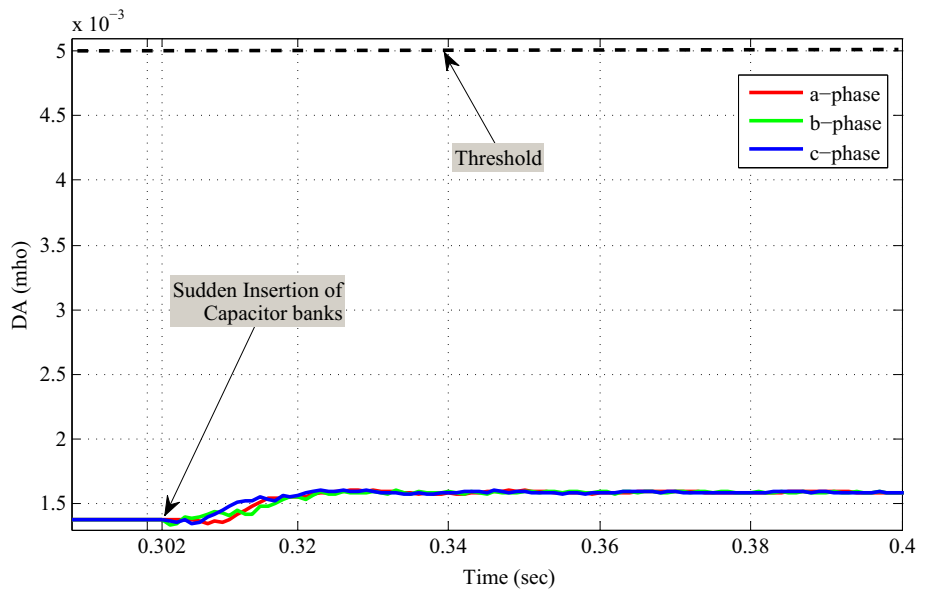
Fig. 8 Plot of per-phase DA for external faults: **a** a–g fault at 0.25 s; **b** a–c–g fault at 0.25 s

Fig. 9 Plot of per-phase DA for sudden insertion of capacitor bank

5.7 Nonlinear Impedance Faults

The proposed scheme was verified for test cases of nonlinear high-impedance faults with transient content in specified FSC-compensated line, and the response of the proposed scheme was still found accurate. One of the test cases of nonlinear high-impedance faults with transient content is depicted in Fig. 10. A two-phase b–c fault was created at 0.202 s instance with nonlinear high fault impedance with transient content. It is seen in Fig. 10 that proposed relay did not mal-operate for this nonlinear high-impedance fault condition.

5.8 Load Encroachment

The proposed scheme was tested for many sudden load encroachment cases up to 300 MW at receiving end of the
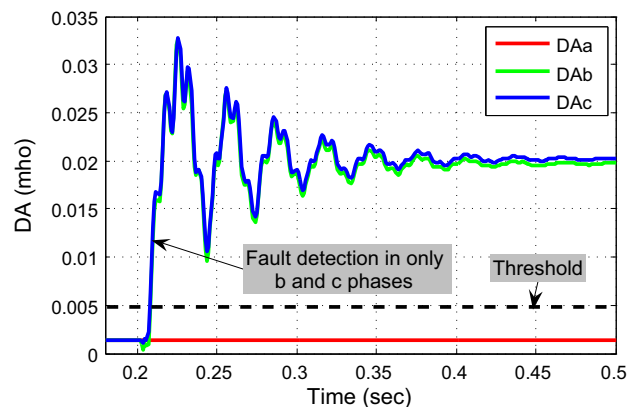

Fig. 10 Plot of per-phase DA for nonlinear high-impedance fault

line and did not mal-operate for these conditions. Figure 11 shows per-phase DA plot for a case of sudden loading of
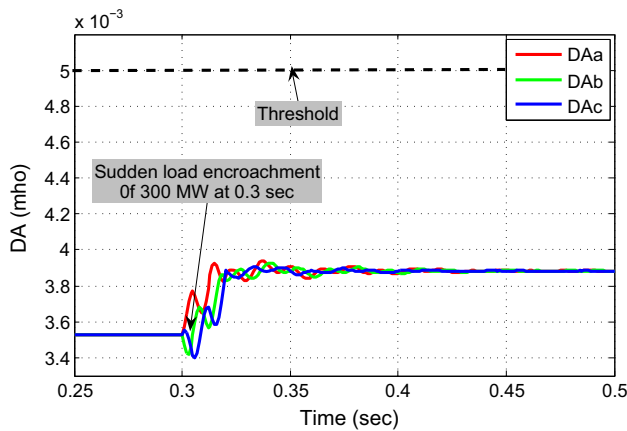
Fig. 11 Plot of per-phase DA for sudden load increment

300 MW at receiving end at 0.3 s with FSC in line. It is seen from Fig. 11 that per-phase DA values were well below the set threshold and proposed scheme was immune to such sudden high-load encroachment.

Tables 2, 3 and 4 give consolidated performance evaluation of the proposed scheme over wide range of fault parameters with simulations. In Tables 2, 3 and 4, the first column gives fault type, the second column gives the fault distance measured from relaying end, the third column shows an instance at which fault was created and last three columns show fault time detection in each phase. *ND* represents no detection of fault in the phase. It was observed that even with variation in different fault parameters, the proposed scheme detected fault accurately with fast response.

6 Algorithm Verification on Hardware

The DA concept has been verified on the laboratory hardware with two-machine system as shown in Fig. 12. The hardware mainly consists of sending-end generator, receiving-end generator, transmission-line module equivalent to 200 km, current sensors and the real-time data recorder. The sending-end generator has manual excitation control with variable-frequency induction motor drive as a prime mover with 2 kW capacity. The sending-end generator acts as reference system for synchronization of two-machine system and works on 50 Hz frequency. The receiving-end generator has onboard automatic voltage controller with closed-loop speed-controlled shunt DC motor as a prime mover with 3 kW capacity. The transmission-line module has four pi-modeled sections, viz., two with 70 km and two with 30 km each. This gives more flexibility for creating faults at various locations manually and checking the algorithm simultaneously. The HIOKI make CT6841 sensors are used for three-phase current measurements. HIOKI make 3390 power analyzer is used as a real-time data recorder for acquiring voltage and current signals from two ends for different fault cases. One-phase and two-phase fault cases can be performed with the availability of four ports on this data recorder. The sampling rate of the real-time data recorder is 10 kHz. More than 200 fault test cases were generated, and based on the rigorous observations, threshold was set to 0.02 in this case. Verification of the proposed algorithm with this setup is done with the following steps:

(1) Different types of faults are created on the transmission system module, and per-phase voltage and

Table 2 Performance investigation

Test results for 40% compensation with FSC at relaying end $R_f = 1\ \Omega$					
Type of fault	Fault distance (km)	Fault created at (s)	Fault detection time (s)		
			a-phase	b-phase	c-phase
a–g	100	0.1	0.109	*ND*	*ND*
	200	0.1	0.110	*ND*	*ND*
	300	0.1	0.109	*ND*	*ND*
a–b	100	0.2	0.210	0.209	*ND*
	200	0.2	0.210	0.210	*ND*
	300	0.2	0.210	0.210	*ND*
a–b–g	100	0.3	0.309	0.310	*ND*
	200	0.3	0.310	0.311	*ND*
	300	0.3	0.310	0.311	*ND*
a–b–c	100	0.4	0.408	0.412	0.407
	200	0.4	0.408	0.412	0.408
	300	0.4	0.408	0.409	0.407

Table 3 Performance investigation

Test results for 25% compensation with FSC at midpoint $R_f = 5\ \Omega$

Type of fault	Fault distance (km)	Fault created at (s)	Fault detection time (s)		
			a-phase	b-phase	c-phase
b–g	100	0.1	*ND*	0.113	*ND*
	190	0.1	*ND*	0.115	*ND*
	300	0.1	*ND*	0.114	*ND*
b–c	100	0.2	*ND*	0.208	0.208
	190	0.2	*ND*	0.209	0.208
	300	0.2	*ND*	0.208	0.207
b–c–g	100	0.3	*ND*	0.308	0.307
	190	0.3	*ND*	0.309	0.308
	300	0.3	*ND*	0.308	0.307
a–b–c	100	0.4	0.407	0.412	0.408
	190	0.4	0.409	0.412	0.408
	300	0.4	0.408	0.412	0.407

Table 4 Performance investigation

Test results for 40% compensation with FSC at receiving end $R_f = 10\ \Omega$

Type of fault	Fault distance (km)	Fault created at (s)	Fault detection time (s)		
			a-phase	b-phase	c-phase
c–g	100	0.55	ND	ND	0.559
	200	0.55	ND	ND	0.560
	300	0.55	ND	ND	0.558
a–c	100	0.65	0.658	ND	0.658
	200	0.65	0.658	ND	0.659
	300	0.65	0.659	ND	0.659
a–c–g	100	0.75	0.760	ND	0.760
	200	0.75	0.758	ND	0.758
	300	0.75	0.758	ND	0.758
a–b–c	100	0.85	0.860	0.862	0.860
	200	0.85	0.859	0.862	0.858
	300	0.85	0.860	0.863	0.861
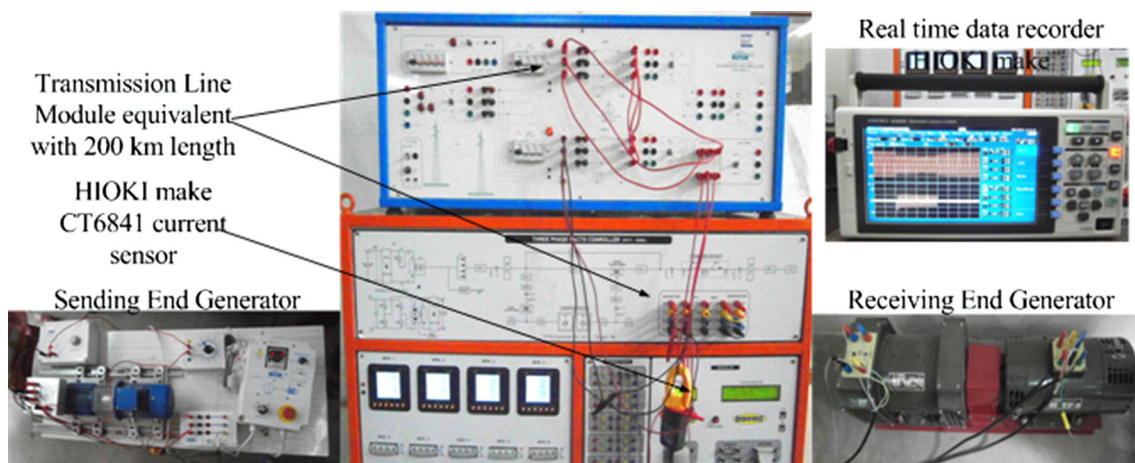
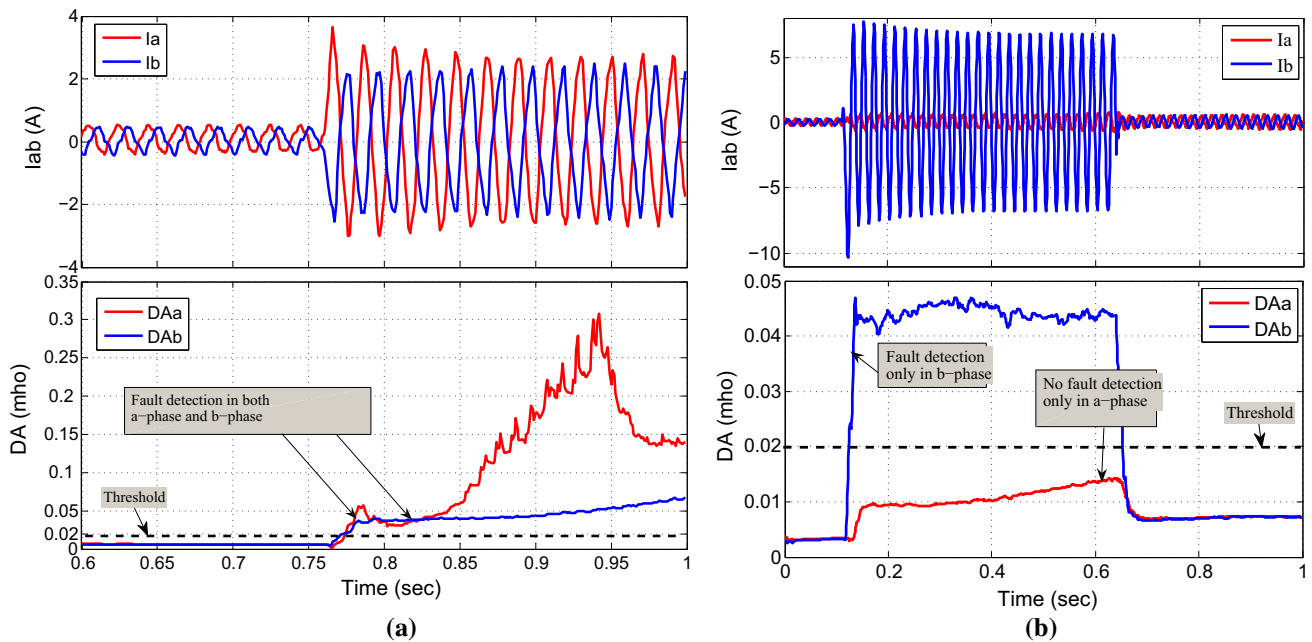**Fig. 12** Hardware setup with two-machine system

Fig. 13 Plots of phase currents and per-phase DA for **a** a–b fault and **b** b–g fault, respectively

current samples from both ends are recorded as input in real-time data recorder.

(2) These gathered input samples in real-time data recorder are then fed to MATLAB program which implements the proposed DA-based relaying algorithm.

(3) Performance of the proposed relaying algorithm is analyzed, and the observations are reported simultaneously.

A large number of faults cases were tested using fault resistances of 0.1 Ω and 1 Ω. Figure 13 shows plots of phase currents (amp) and per-phase DA for (a) a–b fault (170 km from sending end) and (b) b–g fault (100 km from sending end), respectively. It was seen that as soon as the fault occurred, per-phase DA of only faulty phase crossed the threshold and fault was detected in that phase only. For example, in case of b–g fault in Fig. 13b, only DA plot of faulty b-phase was found to cross the set threshold, whereas other phase DA plot did not cross the threshold and hence fault was detected in only a-phase. This showed that the DA concept worked accurately with simulation model as well as with hardware setup proving its accuracy and reliability for implementation in real-time system.

7 Comparative Analysis

Comparative analysis and superiority of the DA-based scheme over recent schemes are as follows:

- There is no need to change the threshold value in uncompensated as well as a series-compensated system in proposed DA-based pilot relaying. However, the concept of fault component-integrated power utilized in reference (Bolandi et al. 2014) has to change the relay threshold value by a multiplying by factor 10 for series-compensated lines. Also, only one installation location and level of series compensation have been considered in (Bolandi et al. 2014).

- When the operating time is considered as a factor of comparison with the recently published work with the availability of same facilities (Bolandi et al. 2014), the detection time for faults with high fault resistance of 50 Ω is found to be 12 ms. However, the proposed work detects faults accurately for fault resistance of 70 Ω in 10 ms as shown in Fig. 5. Even after checking for high fault resistances up to 300 Ω, the proposed relaying algorithm still detects all the faults accurately well within 15 ms.

- Computational burden is very low in proposed DA-based scheme, and it has used a sampling frequency of only 1 kHz achieving faster response. However, schemes in (Shien et al. 2011; Suonan et al. 2011a, b; He et al. 2013a, b) have used sampling frequency of 2 kHz, (Jena and Samantaray 2014a, b) have used 20 kHz and schemes in (Jena and Samantaray 2014a, b) have used 1.2 kHz, respectively, with high computational burden.

- Proposed DA-based scheme works accurately even with uncompensated line and fixed series compensation modes with various compensation locations and %compensation levels. Series compensation effect is not considered in (Suonan et al. 2011a, b) with algorithms based on fault component-integrated impedance approach.

8 Conclusions

In this research paper, a new scheme based on DA has been proposed for fault detection, faulty phase identification and trip decision for EHV 400 kV transmission line of the Western Grid of Power Grid Corporation of India Ltd. with and without FSC compensation. A broad range of fault properties has been tested to produce the training and testing data in order to improve the consistency of the scheme. The proposed relaying algorithm works correctly on a wide range of fault conditions and detects the fault within 15 ms time. The advantage is that scheme does not require any change in the proposed relay threshold settings, even with different FSC installation locations, %compensation levels, sudden load changes which have to be changed in conventional relay settings. This DA concept has never been used before in any of the earlier conventional protection algorithms of lines which make the proposed scheme distinctive. The proposed online scheme, with fast fault detection, ruggedness and least complexity, is a prospective reliable relaying solution to uncompensated as well as FSC-compensated EHV transmission system, and the same will be validated in near future with power grid offline testing. It can be anticipated that the application of DA concept will be applied in relaying to series-compensated EHV transmission system in near future.

Appendix A: Transmission System Parameters

- Line length with FSC—400 km
- External line lengths—300 km
- Thermal limit of quad moose conductor—3000 A
- Conductor type—quad aluminum conductor steel-reinforced (ACSR) moose
- $R_1 = 0.0146$ Ω/km, $X_1 = 0.2530$ Ω/km, $B_1 = 4.5777$ μ-mho/km (positive sequence values)
- $R_0 = 0.2479$ Ω/km, $X_0 = 1.0001$ Ω/km, $B_0 = 2.6345$ μ-mho/km (zero sequence values)
- Bus voltage—400 kV
- Fault MVA level—2.45 GVA
- Frequency—50 Hz

References

Ahmed A, Singh AR, Dambhare S (2012) New modified first zone algorithm for transmission lines with series compensators. In: Fifth IEEE power India conference, Murthal, India

Bolandi TG, Seyedi H, Hashemi SM (2014) Protection of transmission lines using fault component integrated power. IET Gener Transm Distrib 8(12):2163–2172

Chen K, Huang C, He J (2016) Fault detection, classification and location for transmission lines and distribution systems: a review on the methods. High Volt 1(1):25–33

Dambhare S, Soman SA, Chandorkar MC (2009) Adaptive current differential protection schemes for transmission-line protection. IEEE Trans Power Deliv 24(4):1832–1841

Dewadasa M, Ghosh A, Ledwich G (2009) An inverse time admittance relay for fault detection in distribution networks containing DGs. In: TENCON 2009—IEEE Region 10 conference, Singapore

Gupta OH, Tripathy M (2014) An integrated impedance based pilot protection scheme for SVC compensated transmission line. In: IEEE international conference on power, control and embedded systems (ICPCES), Allahabad, India

Gupta Om, Tripathy M (2015) An innovative pilot relaying scheme for shunt compensated line. IEEE Trans Power Deliv 30(3):1439–1448

He S, Suonan J, Bo ZQ (2013a) Integrated impedance-based pilot protection scheme for the TCSC-compensated EHV/UHV transmission lines. IEEE Trans Power Deliv 28(2):835–844

He S, Suonan J, Kang X, Jiao Z (2013b) Fault component integrated impedance-based pilot protection scheme for EHV/UHV transmission line with thyristor controlled series capacitor (TCSC) and controllable shunt reactor (CSR). Sci China Technol Sci 56(2):342–350

Hinge T, Dambhare S (2015) Secure phase comparison schemes for transmission-line protection using synchrophasors. IEEE Trans Power Deliv 30(4):2045–2054

Jena MK, Samantaray SR (2014) Synchrophasor measurement based smart relays for UPFC compensated transmission system. In: Australasian universities power engineering conference, (AUPEC), Perth, WA

Jena MK, Samantaray SR (2014) IPII based intelligent relay for TCSC compensated transmission lines: tested on real time platform. In: IEEE eighteenth national power system conference (NPSC), Guwahati, India

Jena MK, Samantaray SR (2015) Intelligent relaying scheme for series-compensated double circuit lines using phase angle of differential impedance. Int J Electr Power Energy Syst 70:17–26

Jena MK, Samantaray SR (2016) Data-mining-based intelligent differential relaying for transmission lines including UPFC and wind farms. IEEE Trans Neural Netw Learn Syst 27(1):8–17

Kim H, Sohn H, Bricker D (2011) Generation expansion planning using benders' decomposition and generalized networks. Int J Ind Eng Theory Appl Pract 18(1):25–39

Kumar J, Jena P (2019) Fault detection during asymmetrical power swing using superimposed negative sequence current. Arab J Sci Eng 44:7033–7046

Rahmani M, Vinasco G, Rider MJ (2013) Multistage transmission expansion planning considering fixed series compensation allocation. IEEE Trans Power Syst 28(4):3795–3805

Sarangi S, Pradhan AK (2014) Synchronised data-based adaptive backup protection for series compensated line. IET Gener Transm Distrib 8(12):1979–1986

Shien H, JaLe S, Xiaoning K (2011) Fault component integrated impedance-based pilot protection scheme for the TCSC compensated EHV/UHV transmission line. In: IEEE international

conference on advanced power system automation and protection (APAP), Beijing, China

Suonan J, Deng X, Liu K (2011a) Transmission line pilot protection principle based on integrated impedance. IET Gener Transm Distrib 5(10):1003–1010

Suonan J, Liu K, Song G (2011b) A novel UHV/EHV transmission-line pilot protection based on fault component integrated impedance. IEEE Trans Power Deliv 26(1):127–134

Tan Z, Sun H, Nikovski D, Takano T, Kojima Y (2015) A generalized admittance based method for fault location analysis of distribution systems. In: IEEE power & energy society innovative smart grid technologies conference (ISGT), Washington, DC

Vyas B, Maheshwari RP, Das B (2014) Protection of series compensated transmission line: issues and state of art. Electr Power Syst Res 107:93–108